

The genus zero, 3-component fibered links in S^3

Carson Rogers

Abstract

The open book decompositions of the 3-sphere whose pages are pairs of pants have been fully understood for some time, through the lens of contact geometry. The purpose of this note is to exhibit a purely topological derivation of the classification of such open books, in terms of the links that form their bindings and the corresponding monodromies. We construct all of the links and their pair-of-pants fiber surfaces from the simplest example, a connected sum of two Hopf links, through performing (generalized) Stallings twists. Then, by applying the now-classical theory of genus two Heegaard diagrams in S^3 , we verify that the monodromies of the links in this family are the only ones corresponding to pair-of-pants open book decompositions of S^3 .

1 Introduction

Say that an open book decomposition of a closed 3-manifold M is of *type* (g, b) if the pages have genus g and the binding is a b -component link. It comes as no surprise that S^3 admits very few open book decompositions of types (g, b) for some of the smallest values of g and b . Namely, the annular open book decompositions with bindings given by the right and left-handed Hopf links are the only open book decompositions of S^3 of type $(0, 2)$ [1], and the two trefoil knots and the figure-eight knot form the bindings of the only three open book decompositions of type $(1, 1)$ [8].

The next simplest open book decompositions of S^3 are those of types $(0, 3)$, whose pages are pairs of pants. This is an infinite family of open books, and in the proof of Lemma 5.5 of [4], Etnyre and Ozbagci quickly enumerate the monodromies of all examples. Their goal is to describe the corresponding contact structures, and as such, their argument relies on contact geometry. In particular, they rule out a large class of potential monodromies by considering Stein fillings of the corresponding contact 3-manifolds.

Before becoming aware of their work, and with different motivations, the author arrived at the same explicit classification of these open books several years ago, through purely 3-dimensional, topological methods. While experts on fibered links and Heegaard theory likely expect that this is possible to do, it seems that no such argument has appeared in writing outside of the author's PhD thesis. The purpose of releasing this separately is, ideally, to make the result better known to low-dimensional topologists who are not immersed in contact geometry.

We couch the theorem and our proof in the language of fibered links. Say that a $(b$ -component) fibered link in S^3 is of *type* (g, b) if it forms the binding of an open book decomposition of that type.

Theorem 1.1. *The fibered links in S^3 of type $(0, 3)$ consist of connected sums of Hopf links, the links L_n of Figure 1, the link depicted in Figure 2, and its mirror image. The fiber surfaces of any two of these links are related by a sequence of Stallings twists.*

The second statement of this theorem is a byproduct of the most natural way of constructing the fiber surfaces of these links, so as to identify their monodromies. Here, we take the definition of a Stallings twist given by Harer [9], in which the twisting curve on the fiber surface is allowed to have

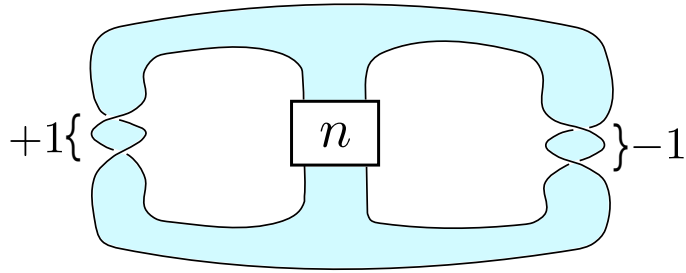


Figure 1: The links L_n , together with their genus zero fiber surfaces.

framing 0 or ± 2 . Following explicit descriptions of the monodromies of the links listed here, we prove that no other automorphism of a pair of pants can arise as the monodromy of such a fibered link in S^3 by analyzing the corresponding genus two Heegaard diagrams.

We note that the only redundancy to occur in our listing of these links is L_0 , which is a connected sum of two Hopf links of opposite type. It is no accident that all of these links contain a Hopf sub-link: if L is a 3-component link in a 3-manifold M whose exterior is fibered by pairs of pants, then L contains the exceptional fibers of a Seifert fibering of M over S^2 .

The paper is organized as follows. In Section 2, we give background and definitions. In Section 3.1, we provide constructions of the links described above which prove that they are fibered and of genus zero, when given appropriate orientations. In Section 3.2, we then use the theory of genus two Heegaard diagrams in S^3 to show that any fibered link in S^3 of type $(0, 3)$ must have the same monodromy as one of these links.

2 Preliminaries

All manifolds under consideration are assumed to be orientable. Isotopies of embedded objects in a 3-manifold M are always taken to be proper when $\partial M \neq \emptyset$. Two links or embedded surfaces in M will be regarded as the same if they are (properly) isotopic. If L is a link in M , we use M_L to denote the compact exterior $\overline{M - \eta(L)}$ of L in M , where $\eta(L)$ is a tubular neighborhood of L in M . For basic terminology and facts from 3-manifold topology that are taken for granted throughout, we refer the reader to [13].

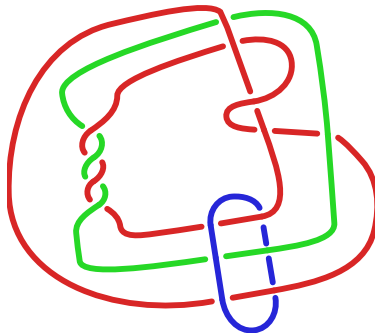


Figure 2: One of the two exceptional fibered links of type $(0, 3)$, the other being its mirror image.

2.1 Fibered links

Let L be an oriented null-homologous link in a closed, oriented 3-manifold M . A *Seifert surface* for L is an embedded compact, oriented surface F in M such that $\partial F = L$. We can equally well regard a Seifert surface as being properly embedded in M_L , and the two viewpoints will be used interchangeably. We say that L is *fibered* if $E(L)$ fibers over S^1 , so that the fiber F is a Seifert surface for L . We say that F is a *fiber surface* for L . When speaking of a fiber surface without reference to a specific link, we mean a fiber surface for some fibered link in M . A compact, orientable surface is said to be of *type* (g, b) if it has genus g and b boundary components. A fibered link in M is said to be of type (g, b) if its fiber surface is of type (g, b) .

If L is a fibered link with fiber surface F , then M_L may be realized as a mapping torus $F \times [0, 1] / ((x, 1) \sim (\phi(x), 0))$, where $\phi : F \rightarrow F$ is a homeomorphism which fixes ∂F pointwise. We say that ϕ is a *monodromy* for F . Note that a monodromy for F is defined up to isotopy and conjugation by other self-homeomorphisms of F .

Conversely, given a surface with boundary F and an orientation-preserving homeomorphism $\phi : F \rightarrow F$ which fixes ∂F pointwise, there is a canonical way [3] to fill in the boundary of the mapping torus of ϕ with solid tori V_1, \dots, V_n to obtain a closed 3-manifold M_ϕ . The cores of V_1, \dots, V_n then constitute a well-defined link L_ϕ in M_ϕ , which is denoted by B_ϕ in [3].

Product disks. Let L be a fibered link in M with fiber surface F , and let $\eta(F) \cong F \times I$ be a closed regular neighborhood of F in M_L such that $F \times \{t\}$ is a fiber of the fibration of M_L for each $t \in I$. The surface exterior $M_F = \overline{M_L} - N(F)$ has a corresponding parametrization as $F \times I$. A *product disk* is in $\eta(F)$ or M_F is a properly embedded disk D such that ∂D intersects each component of $F \times \partial I$ in a single properly embedded arc. A product disk may be isotoped so that it intersects each fiber $F \times \{t\}$ in a single arc.

A monodromy ϕ for F defines a natural pairing between product disks in $\eta(F)$ and those in M_F . Viewing M_L as the quotient of $F \times [0, 1]$ by the action of ϕ , we take $F \times [0, 1/2]$ to be $\eta(F)$ and $F \times [1/2, 1]$ to be M_F . Up to isotopy, every product disk in $\eta(F)$ is uniquely realized as $D(\alpha) = \alpha \times [0, 1/2]$ for some properly embedded arc α in F . The same is true in M_F , with $[0, 1/2]$ replaced by $[1/2, 1]$. Since $(x, 1)$ is identified with $(\phi(x), 0)$ to form M_L , we denote $\alpha \times [1/2, 1]$ by $D(\phi(\alpha))$. Once perturbed to lie in general position, $\partial D(\alpha)$ and $\partial D(\phi(\alpha))$ will typically intersect non-trivially.

Fiber surfaces of type (0,3). The types of fiber surfaces to be considered here, with their monodromies, are naturally enumerated by multisets of three integers. Let F be an oriented pair of pants, an abstract surface of type $(0, 3)$, with boundary components labeled b_1, b_2, b_3 . For each $i = 1, 2, 3$, let c_i be a simple closed curve embedded in $\text{Int}(F)$ which is parallel to b_i . Assume that c_1, c_2, c_3 have been chosen to be mutually disjoint. Throughout, we let T_i denote a left Dehn twist along c_i , according to the convention of Figure 3. The inverse T_i^{-1} is then a right twist along c_i . The composition of $T_i^{n_i}$ and $T_j^{n_j}$ will be denoted by $T_i^{n_i} T_j^{n_j}$. Note that, since the three curves are mutually disjoint, T_i always commutes with T_j .

The mapping class group of F is isomorphic to \mathbb{Z}^3 [5], with an explicit isomorphism given by sending the isotopy class of T_i to the i^{th} standard unit vector $e_i = (\delta_{1i}, \delta_{2i}, \delta_{3i})$. Every orientation-preserving homeomorphism $\phi : F \rightarrow F$ which fixes ∂F pointwise is therefore isotopic to a unique homeomorphism of the form $T_1^{n_1} \circ T_2^{n_2} \circ T_3^{n_3}$. The manifold-link pair (M_ϕ, L_ϕ) is then determined by the triple n_1, n_2, n_3 .

Further, if $\{n_1, n_2, n_3\} = \{n'_1, n'_2, n'_3\}$, then the mapping tori of $\phi = T_1^{n_1} T_2^{n_2} T_3^{n_3}$ and $\phi' = T_1^{n'_1} T_2^{n'_2} T_3^{n'_3}$ are exactly the same, up to relabeling the boundary components of F . The pairs (M_ϕ, L_ϕ) and $(M_{\phi'}, L_{\phi'})$ are therefore the same. From this point forward, we denote this pair by

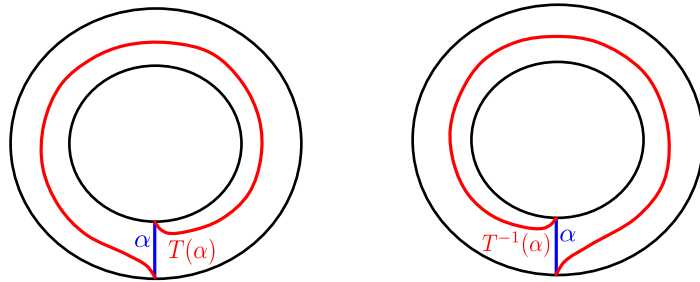


Figure 3: Standard conventions for right and left-handed Dehn twists (right and left, resp.)

$(M[n_1, n_2, n_3], L[n_1, n_2, n_3])$, understanding that the order of n_1 , n_2 , and n_3 is unimportant. The associated fiber surface for $L[n_1, n_2, n_3]$ will likewise be denoted by $F[n_1, n_2, n_3]$.

Stallings twists. Stallings twists are operations by which new fiber surfaces in S^3 can be produced from old ones. They were introduced by Stallings in [14], and will be used to construct the fibered links appearing in the statement of the main theorem. The version described here is a slight generalization of Stallings' original definition which appears in [9].

Let F be an oriented fiber surface in S^3 bounded by a link L , and let c be an essential closed curve embedded in F which is unknotted in S^3 . Suppose that $lk(c, c^+) + \delta_1 = \delta_2$, where c^+ is a copy of c pushed off of F to the positive side, $\delta_1 = \pm 1$, and $\delta_2 = \pm 1$. Let A be a regular neighborhood of c in F and N be a solid torus obtained by thickening A to the positive side of F . We choose N so that a neighborhood of c^+ in the corresponding fiber lies in ∂N , and the restriction of the fibration of $S^3 - L$ to N is a product fibration by annuli.

To obtain a new fiber surface from F , perform Dehn surgery on S^3 along the core of N by removing N and regluing it by the homeomorphism of the boundary torus illustrated in Figure 4. This map sends a meridian of N which intersects c^+ once transversely to a Haken sum of itself with c^+ . The choice of which way to resolve the point of intersection depends on δ_1 : we resolve it so that one 'turns left' into the meridian after traversing c^+ if $\delta_1 = -1$, and 'turns right' into the meridian if $\delta_1 = +1$.

It follows that the surgery coefficient is $\delta_2 = \pm 1$, so the resulting 3-manifold is S^3 . The key point is that this procedure turns F into a new fiber surface F' , bounded by some link L' . Away from N , the fibration of the exterior of L' will agree with that of the exterior of L . The restriction of the fibration to N will again be a product fibration of N by annuli, two being neighborhoods of c and c_+ in ∂N . If h is a monodromy for F , then $h \circ T_c^{\delta_1}$ is a monodromy for F' , where T_c denotes a left-handed Dehn twist along c .

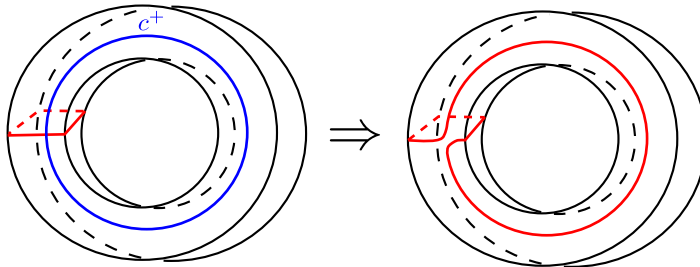


Figure 4: Re-gluing map for the solid torus N which defines a Stallings twist.

Definition 2.1. In the above situation, we say that F' is obtained from F by performing a *Stallings twist of type ϵ* on F along c , where $\epsilon = \frac{1}{2}lk(c, c^+)$. We also say that c is a *Stallings curve of type ϵ* with respect to F . A Stallings twist will be called *positive* (resp. *negative*) if the surgery coefficient δ_2 is $+1$ (resp. -1).

Note that the condition $lk(c, c^+) + \delta_1 = \delta_2$ means that ϵ is either 0 or ± 1 . While a Stallings twist of type 0 can be either positive or negative, those of type 1 are necessarily negative, while those of type -1 must be positive. If F' is obtained from F by performing a Stallings twist of type ϵ along c , then F is evidently obtained from F' by performing a Stallings twist of type $-\epsilon$ along c , where c is now viewed as a curve embedded in F' in the natural sense.

A final observation is that a Stallings twist of type 0 may be iterated. If c is a Stallings curve of type 0 in F and F' is obtained from F by performing a Stallings twist along c , then c is again a Stallings curve of type 0 in F' . It therefore makes sense to speak of performing a positive or negative Stallings twist along c n times in succession for any $n > 0$.

Definition 2.2. Suppose that F is a fiber surface in S^3 and c is a Stallings curve of type 0 in F . If F' is the fiber surface obtained from F by performing $n > 0$ successive positive (resp. negative) Stallings twists along c , then we say that F' is obtained from F by performing a *Stallings n -twist* (resp. *$-n$ -twist*) along c .

By induction and our previous observation on the effect of a Stallings twist on the monodromy, one sees that if F' is obtained from F by performing a Stallings n -twist along c and h is a monodromy for F , then $h \circ T_c^n$ is a monodromy for F' .

2.2 Genus two Heegaard diagrams

Throughout this subsection, Σ will denote a closed, orientable surface of genus two. A *curve* in Σ will always refer to a simple closed curve embedded in Σ . Every curve under consideration is assumed to be *essential*, meaning that it does not bound an embedded 2-disk in Σ . Whenever discussing a collection of two or more curves in Σ , we always assume that they have been isotoped so that every pair intersects transversely in a finite number of points. Upon orienting two curves c_1 and c_2 in Σ , we may consider the algebraic intersection number of c_1 with c_2 , denoted $c_1 \cdot c_2$, by counting the signed number of intersection points of c_1 with c_2 .

A *cut system* for Σ is a pair α of disjoint curves α_1 and α_2 which cut Σ into a planar surface, denoted by Σ_α , with four boundary components. A (genus two) *Heegaard diagram* (Σ, α, β) consists of two cut systems α and β for Σ . We typically suppress Σ and denote the Heegaard diagram by (α, β) . Given a Heegaard diagram (α, β) , we may construct a closed 3-manifold N from $\Sigma \times [-1, 1]$ by attaching one pair of 3-dimensional 2-handles along $\alpha \times \{-1\}$ and another along $\beta \times \{1\}$, and then capping off the resulting 2-sphere boundary components with 3-balls. We then say that (α, β) is a *Heegaard diagram for N* .

Recall that a *Heegaard surface* for a 3-manifold M is a closed, orientable, separating surface Σ embedded in M such that the closure of each component of $M - \Sigma$ is a handlebody. In the above construction, the surface $\Sigma = \Sigma \times \{0\}$ is a genus two Heegaard surface for the 3-manifold N . Conversely, every closed 3-manifold admitting a genus two Heegaard surface arises from a Heegaard diagram via this construction.

Heegaard diagrams from fibered links. Let L be a fibered link in a 3-manifold M with fiber surface F . The boundary of a regular neighborhood of F in M divides M into two copies of the handlebody $F \times I$, and is therefore a Heegaard surface for M . Given a monodromy ϕ for F , a corresponding Heegaard diagram can be constructed from product disks as follows. As before, let $\eta(F) \cong F \times [-1, 1]$

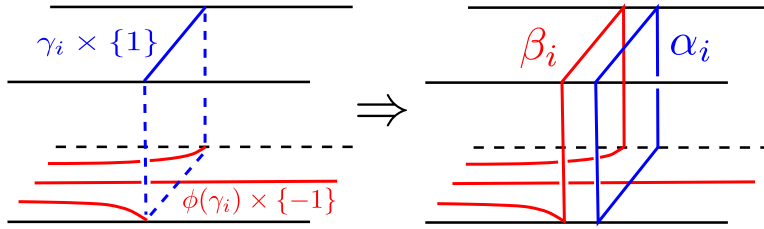


Figure 5: Constructing a pair of curves in a Heegaard diagram defined by the monodromy of a fiber surface.

be a closed regular neighborhood of F in M_L , and let $\eta(F) = \overline{M_L - N(F)}$. Choose a collection of mutually disjoint arcs $\gamma_1, \dots, \gamma_n$ properly embedded in F which cut F into a disk. Assume that $\phi(\gamma_i)$ has been isotoped to intersect γ_i transversely in the fewest possible points for each i .

Let $\gamma'_1, \dots, \gamma'_n$ be nearby parallel copies of $\gamma_1, \dots, \gamma_n$ in F such that $\gamma'_i \cap \gamma_j = \emptyset$ for all i and j . For each i , we assume that γ'_i has been chosen to intersect $\phi(\gamma_j)$ in the fewest possible points for every j . In particular, if $\phi(\gamma_i)$ lies on the same side of γ_i near each endpoint, we choose γ'_i so that it lies on the other side of γ_i .

For each $i = 1, \dots, n$, we define α_i to be the boundary of the product disk $D(\gamma'_i) \subset N(F)$ and β_i to be the boundary of $D(\phi(\gamma_i)) \subset E(F)$. Thus, with respect to the product structure on $N(F)$, we have

$$\alpha_i = (\gamma'_i \times \{-1, 1\}) \cup (\partial\gamma'_i \times [-1, 1]), \quad \beta_i = (\gamma_i \times \{1\}) \cup (\partial\gamma_i \times [-1, 1]) \cup (\phi(\gamma_i) \times \{-1\}).$$

An example construction of one pair α_i, β_i is shown in Figure 5. By construction, both $\alpha = \{\alpha_1, \dots, \alpha_n\}$, and $\beta = \{\beta_1, \dots, \beta_n\}$ are cut systems for $\Sigma = \partial N(F)$, so (Σ, α, β) is a Heegaard diagram for M . We say that such a Heegaard diagram is *associated with* ϕ .

Two fundamental facts about Heegaard diagrams will be required. The ensuing discussion follows parts of Section 2 of [11]. To state the first, let (α, β) be a Heegaard diagram for a 3-manifold M , and let $\alpha = \{\alpha_1, \alpha_2\}$, $\beta = \{\beta_1, \beta_2\}$. Once the four curves have been oriented in some fashion, we consider the *intersection matrix*

$$M(\alpha, \beta) = \begin{pmatrix} \alpha_1 \cdot \beta_1 & \alpha_1 \cdot \beta_2 \\ \alpha_2 \cdot \beta_1 & \alpha_2 \cdot \beta_2 \end{pmatrix}.$$

This as a presentation matrix for the abelian group $H_1(M)$. One can see this through the description of cellular homology in terms of the handle decomposition of M corresponding to the Heegaard diagram (see Section 4.2 of [7]).

Consequently, if $H_1(M)$ is finite, then $|\det M(\alpha, \beta)|$ is equal to the order of $H_1(M)$. In particular, we have:

Lemma 2.1. [11] *If (α, β) is a Heegaard diagram for S^3 , then $|\det M(\alpha, \beta)| = 1$.*

We need some additional definitions. From this point forward, when considering two collections of curves in Σ , we assume that each curve in one collection has been isotoped to intersect each curve in the other in the fewest possible points. Thus, given a cut system $\alpha = \{\alpha_1, \alpha_2\}$ for Σ and a collection \mathcal{C} of mutually disjoint curves which are distinct from α_1 and α_2 , we assume that the intersection of \mathcal{C} with the cut surface Σ_α is a collection of properly embedded, essential arcs.

Whitehead graphs and waves. Let α and \mathcal{C} be as above. Viewing the boundary components of Σ_α as four fat vertices and the components of $\mathcal{C} \cap \Sigma_\alpha$ as edges, we may regard $\mathcal{C} \cap \Sigma_\alpha$ as a topological

graph $\Sigma_\alpha(\mathcal{C})$, called the *Whitehead graph* of \mathcal{C} with respect to α . Examples can be found in Figures 10, 11, and 12 of the following section.

Define a *wave* in Σ_α to be an essential, properly embedded arc whose endpoints both lie in the same component of $\partial\Sigma_\alpha$. Given a Heegaard diagram (α, β) , an α -*wave* for (α, β) is a wave ω properly embedded in Σ_α such that $\omega \cap \beta = \emptyset$. One similarly defines a β -*wave* in Σ_β . If such an arc exists, we say that (α, β) contains a wave *based in* α (resp. β) and that $\Sigma_\alpha(\beta)$ (resp. $\Sigma_\beta(\alpha)$) *contains a wave*.

Our reason for considering waves in Heegaard diagrams is the following theorem of Homma, Ochiai, and Takahashi.

Theorem 2.1. [10] *Every genus two Heegaard diagram (α, β) for S^3 contains either an α -wave or a β -wave.*

The second half of our main proof to follow amounts to a direct application of this result, together with Lemma 2.1. It is a testament to the special nature of genus two Heegaard diagrams, as higher-genus Heegaard diagrams for S^3 need not contain any waves [12].

3 Proof of Theorem 1.1

Our proof breaks into two main parts. In Section 3.1, we prove that the links listed in the statement of Theorem 1.1 are indeed fibered links of type $(0, 3)$. We further show that the fiber surfaces of any two of these links are related by a sequence of Stallings twists, and describe their monodromies explicitly. In Section 3.2, we use the elements of Heegaard theory discussed in Section 2.2 to show that a fibered link of type $(0, 3)$ in S^3 must have the same monodromy as one of these links. Since the monodromy determines the fiber surface up to isotopy [1], this completes the proof.

3.1 Describing the fibrations

The links listed in the statement of Theorem 1.1 are known to be fibered links of type $(0, 3)$. The links L_n of Figure 1 are discussed in [6], and the example of Figure 2 is exhibited in [2] as the result of what the authors refer to as a generalized Hopf banding. However, we give a complete analysis, culminating in the needed descriptions of the monodromies of these links.

Our starting points are the basic facts that the right and left-handed Hopf links are both fibered links, with annular fiber surfaces, and that a boundary-connected sum of two fiber surfaces is again a fiber surface [6]. It follows immediately that all connected sums of two Hopf links are fibered links of type $(0, 3)$, since their fiber surfaces are boundary-connected sums of two annuli.

The annular fiber surface of a Hopf link will be referred to as a *Hopf annulus*. The Seifert surface of the link L_n depicted in Figure 1 is obtained from a boundary-connected sum of two Hopf annuli of opposite types by performing a Stallings $-n$ -twist along the curve shown on the left-hand side of Figure 6, which is readily seen to be a Stallings curve of type 0. The reader can check that the result of pushing this curve off of the surface to either side is isotopic to that appearing on the right-hand side of the figure, surrounding the central band. Performing the $-n$ -twist along the left-hand curve is therefore equivalent to performing $-1/n$ Dehn surgery along that on the right. The result of doing so is precisely the surface depicted in Figure 1, so we conclude that it is a fiber surface.

It remains to prove that the link L of Figure 2 and its mirror image \bar{L} bound fiber surfaces of type $(0, 3)$. Both can be constructed by performing Stallings twists on the fiber surfaces of L_3 and L_{-3} . To obtain the fiber surface for L , perform a positive Stallings twist on the fiber surface for L_3 along the red curve shown on the left of Figure 7, which is a Stallings curve of type -1. The effect of the twist on

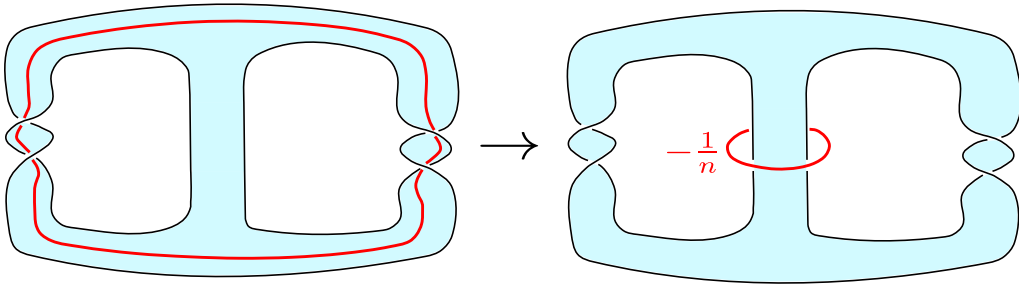


Figure 6: Constructing the fiber surface for L_n of Figure 1 by performing a Stallings n -twist.

the link can be seen by carefully blowing down this curve in the sense of Kirby calculus [7], viewed with framing equal to the surgery coefficient of $+1$. Doing so and simplifying yields the diagram of Figure 2.

The fiber surface for \bar{L} is similarly obtained by performing a negative Stallings twist on the fiber surface for L_{-3} along the curve shown on the right of Figure 7. Since the total 4-component diagram is the mirror image of the previous one and the slope for the surgery curve is -1 , it follows that the resulting link is indeed \bar{L} . This can also be seen from the fact, to be noted shortly, that the monodromies of this fiber surface and that of L are inverse to each other.

To set the stage for Part 2 of our proof, we determine the monodromies of all links examined above. Recall the notation $(M[n_1, n_2, n_3], L[n_1, n_2, n_3])$ for the manifold-link pair determined by the triple of integers n_1, n_2, n_3 , as introduced in Section 2.1. This means that $L[n_1, n_2, n_3]$ is the fibered link of type $(0, 3)$ in $M[n_1, n_2, n_3]$ whose fiber surface has monodromy of the form $T_1^{n_1} T_2^{n_2} T_3^{n_3}$, where c_1, c_2 , and c_3 are disjoint curves in the fiber parallel to its distinct boundary components and T_i is a left-handed Dehn twist along c_i . For simplicity, we will denote this monodromy by $\phi[n_1, n_2, n_3]$. For the present discussion, we choose the labeling of c_1, c_2 , and c_3 relative to the diagrams of Figures 6 and 7 as shown in Figure 8. However, as discussed in Section 2.1, $[n_1, n_2, n_3]$ should really be regarded as a multiset of three integers, rather than an ordered triple.

In the case of a boundary-connected sum of two Hopf annuli, our convention is such that c_3 is the only curve which intersects both summands. Since the monodromy of a right-handed (resp. left-handed) Hopf annulus is a left (resp. right) Dehn twist about its core curve, it follows that the monodromy for a boundary-connected sum of two Hopf annuli is $\phi[\pm 1, \pm 1, 0]$, as its restriction to each summand must be the monodromy of that summand [6]. When the two Hopf annuli are of opposite types, as on the left of Figure 6, the monodromy is $\phi[1, -1, 0]$. It then follows from the above construction of the links L_n , via the final remark of Section 2.1, that the monodromy for the fiber surface

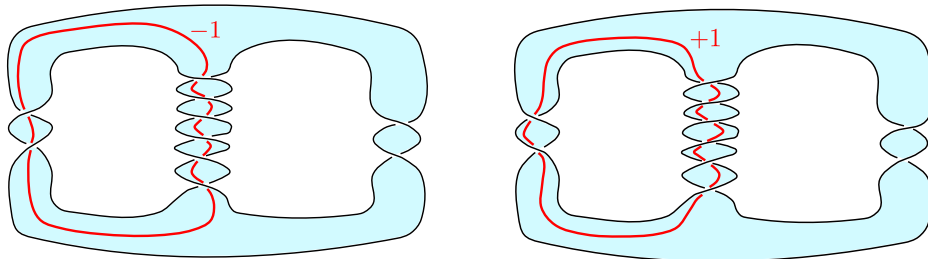


Figure 7: Constructing the fiber surfaces for the link of Figure 2 (left) and its mirror image (right) via Stallings twists of types -1 and 1 .

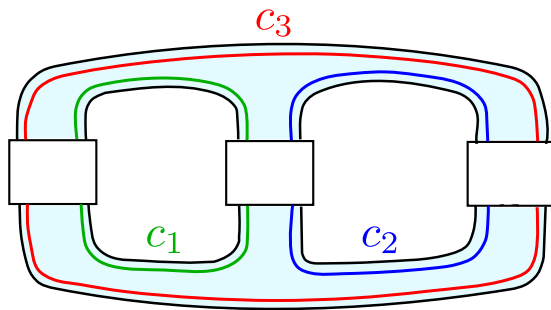


Figure 8: Labeling of the three essential curves in a surface of type $(0,3)$ used to write down monodromies of the fiber surfaces in the main theorem.

of L_n is given by $\phi[1, -1, -n]$. Likewise, by our construction of the remaining two fiber surfaces of type $(0,3)$ from those of L_{-3} and L_3 via Stallings twists, it follows that their monodromies are given by $\phi[2, -1, 3]$ and $\phi[-2, 1, -3]$ (respectively).

Using the above observations, we can now show that any two of the above links are related by a sequence of Stallings twists. So far, we have seen that the fiber surfaces of the links L_n , L , and \bar{L} can be constructed from that of L_0 by a sequence of Stallings twists. The claim therefore reduces to showing that a boundary-connected sum of two Hopf annuli of the same type is related to the fiber surface of one of these links by a sequence of Stallings twists. In fact, one twist will suffice. Letting F denote one of these two surfaces, a curve c in F parallel to the boundary component which meets both of the Hopf annulus summands will be a Stallings curve of type 1 if they are right-handed, and type -1 if they are left-handed. Performing the corresponding Stallings twist produces a fiber surface with monodromy $\phi[1, 1, -1] = \phi[1, 1, 0] \circ T_c^{-1}$ in the first case, and one with monodromy $\phi[-1, -1, 1] = \phi[-1, -1, 0] \circ T_c$ in the second. It follows from the above discussion that the resulting fiber surfaces are those of L_{-1} and L_1 (respectively). We have therefore proven the second statement of Theorem 1.1.

3.2 The list is complete

It remains to show that we have described all fibered links of type $(0,3)$. By the work done in Section 3.1, it suffices to prove that $M[n_1, n_2, n_3] \cong S^3$ only if $[n_1, n_2, n_3]$ is one of $[\pm 1, \pm 1, 0]$, $[2, -1, 3]$, $[-2, 1, -3]$, or $[1, -1, n]$. To begin, note that $M[-n_1, -n_2, -n_3]$ is related to $M[n_1, n_2, n_3]$ by an orientation-reversing homeomorphism which takes $L[-n_1, -n_2, -n_3]$ to $L[n_1, n_2, n_3]$, as the corresponding monodromies are inverse to each other. We may consequently assume that at least two of the integers, say n_1 and n_3 , are nonnegative.

If one of the n_i is zero, then the monodromy for $F[n_1, n_2, n_3]$ fixes an essential, separating arc, revealing a 2-sphere which decomposes $F[n_1, n_2, n_3]$ as the boundary-connected sum of two annular fiber surfaces. If $M[n_1, n_2, n_3] \cong S^3$, this means that $F[n_1, n_2, n_3]$ is a boundary-connected sum of two Hopf annuli, in which case $[n_1, n_2, n_3] = [\pm 1, \pm 1, 0]$. Thus, we need only consider the case that n_1 and n_3 are strictly positive. If in addition $n_2 = -1$, we already know that $M[n_1, n_2, n_3] \cong S^3$ if either $n_1 = 1$ or $n_3 = 1$, as $M[n_1, n_2, n_3]$ is then $M[1, -1, n]$ for some n . It therefore suffices to prove the following.

Proposition 3.1. (a) If $n_1 > 0$, $n_3 > 0$, and $M[n_1, n_2, n_3] \cong S^3$, then $n_2 = -1$.

(b) If $n_2 = -1$ and $1 < n_1 \leq n_3$, then $M[n_1, n_2, n_3] \cong S^3$ if and only if $n_1 = 2$ and $n_3 = 3$.

Part (b) of this proposition will be established in Lemma 3.1 by applying Lemma 2.1. There, we

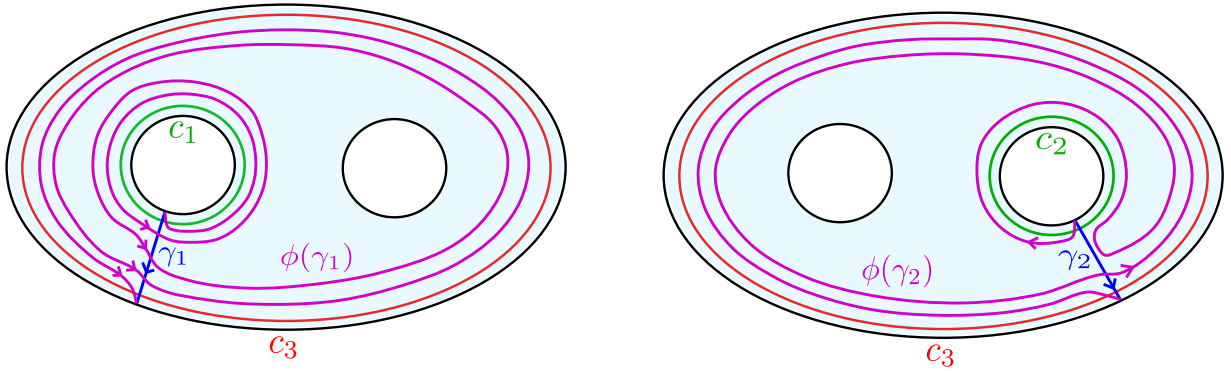


Figure 9: Images of the arcs γ_1 and γ_2 under $\phi = T_1^2 T_2^{-1} T_3^2$.

also take the first step towards proving (a) by showing that $n_2 < 0$ if both n_1 and n_3 are positive. We then complete the proof (a) by applying Theorem 2.1.

For what follows, F will denote the (abstract) surface of type $(0, 3)$, with push-offs of its boundary components labeled c_1, c_2, c_3 in some fashion. In the above notation, this labeling yields a description of the monodromy of $L[n_1, n_2, n_3]$ as $\phi[n_1, n_2, n_3] = T_1^{n_1} T_2^{n_2} T_3^{n_3}$. Let γ_1 and γ_2 be mutually disjoint arcs properly embedded in F such that γ_i runs from the boundary component parallel to c_i to that parallel to c_3 . We consider the genus two Heegaard diagram (α, β) determined by $\phi[n_1, n_2, n_3]$, as defined in Section 2.2. Recall that we are assuming both n_1 and n_3 to be positive.

We first describe the action of $\phi = \phi[n_1, n_2, n_3]$ on γ_1 and γ_2 . As described in [5] in a more general setting, the process of computing $\phi(\gamma_i)$ may be viewed as taking $|n_j|$ parallel copies of c_j for each $j = 1, 2, 3$ and resolving their points of intersection with γ_i in the appropriate manner, as determined by the sign of each n_j . In both cases, after $\phi(\gamma_i)$ is computed in this fashion and perturbed very slightly, it will intersect both γ_1 and γ_2 in the fewest possible number of points. The computations for the case $n_1 = 2 = n_3, n_2 = -1$ are shown in Figure 9. Note that, under the conventions indicated in that figure, $\phi(\gamma_i)$ will intersect γ_i in $|n_i| + n_3$ points.

Let (Σ, α, β) denote the Heegaard diagram associated with ϕ determined by the pair γ_1, γ_2 , as defined in Section 2.2. We begin by using the intersection matrix $M(\alpha, \beta)$ to obtain some basic restrictions on the triple n_1, n_2, n_3 needed for $M[n_1, n_2, n_3]$ to be S^3 . In particular, we prove part (b) of Proposition 3.1.

Lemma 3.1. *Let $M[n_1, n_2, n_3]$ be the 3-manifold defined above. Suppose that n_1 and n_3 are strictly positive and $M[n_1, n_2, n_3] \cong S^3$. If $n_2 \neq 0$, then n_2 must be negative. Further, if $n_2 = -1$ and $1 < n_1 \leq n_3$, then $n_1 = 2$ and $n_3 = 3$.*

Proof. Let (Σ, α, β) be as above. To write down $M(\alpha, \beta)$, for both $i = 1, 2$, orient both γ_i and $\phi(\gamma_i)$ so that their terminal endpoints lie on the boundary curve parallel to c_3 . Orient the corresponding curves α_i and β_i in the Heegaard diagram accordingly.

As visible in Figure 5 of Section 2.2, for both $i = 1, 2$, the points in which α_i and β_i intersect all lie in the lower copy $F \times \{-1\} \subset \Sigma$ of the fiber surface. In fact, they correspond exactly to the $|n_i| + n_3$ points of intersection of γ_i with $\phi(\gamma_i)$ if n_i is positive, endpoints included, while they correspond to the interior points of intersection of the two arcs if n_i is negative. In the former case, as illustrated on the left side of Figure 9, the sign of each intersection point of γ_i with $\phi(\gamma_i)$ is $+$ when the unit tangent vector to γ_i is taken as the first vector in the corresponding basis of the tangent space. Since

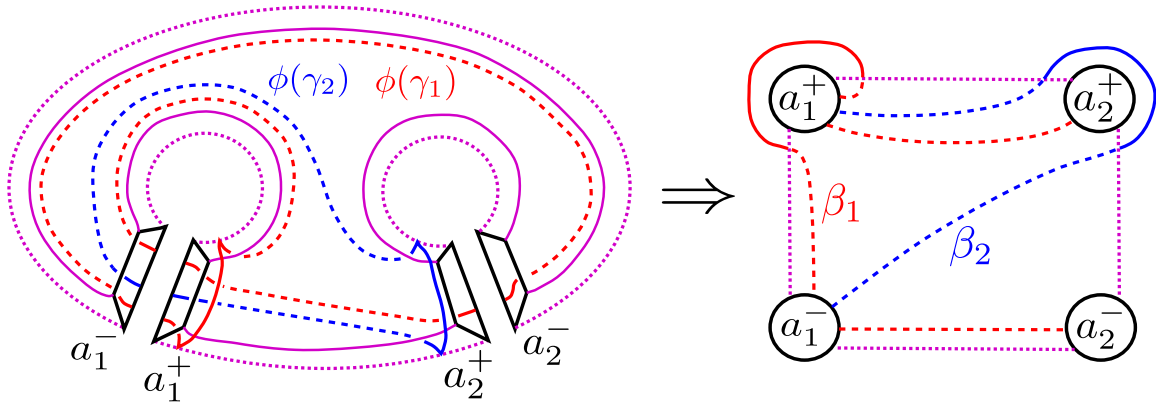


Figure 10: Using $\phi(\gamma_1)$ and $\phi(\gamma_2)$ to draw the Whitehead graph for (α, β) . On the left, the dashed arcs should be thought of as sitting in $F \times \{-1\} \subset \Sigma = \partial(F \times [-1, 1])$, with the solid arcs lying above them. The dotted purple arcs lie in the boundary of $F \times \{-1\}$, and are not part of the Whitehead graph.

the signs of these points are the same as the signs of the corresponding intersection points of α_i with β_i , this means that $\alpha_i \cdot \beta_i = |\gamma_i \cap \phi(\gamma_i)| = n_i + n_3$ when n_i is positive.

It also turns out that $\alpha_i \cdot \beta_i = n_i + n_3$ when n_i is negative. Here, while α_i intersects β_i in two fewer points, the pair of points of $\gamma_i \cap \phi(\gamma_i)$ that have been removed are the endpoints. Since n_i is negative while n_3 is positive, these have opposite signs. The signs of the points of $\text{Int}(\gamma_i) \cap \text{Int}(\phi(\gamma_i))$, measured as before, match the signs of the corresponding points of $\alpha_i \cap \beta_i$. This means that $\alpha_i \cdot \beta_i$ is still equal to the sum of the signs of the points of $\gamma_i \cap \phi(\gamma_i)$. The first $|n_i|$ of these points encountered as γ_i is traversed, including the initial endpoint, all have negative sign, while the final n_3 intersection points all have positive sign. Thus, we have $\alpha_i \cdot \beta_i = -|n_i| + n_3 = n_i + n_3$.

It follows from our orientation conventions that the remaining two entries $\alpha_1 \cdot \beta_2$ and $\alpha_2 \cdot \beta_1$ of $M(\alpha, \beta)$ are both equal to n_3 , since $n_3 > 0$. By the observations of the previous two paragraphs, we therefore have

$$M(\alpha, \beta) = \begin{pmatrix} n_1 + n_3 & n_3 \\ n_3 & n_2 + n_3 \end{pmatrix}$$

regardless of the sign of n_2 . By Lemma 2.1, the fact that $M[n_1, n_2, n_3] \cong S^3$ implies

$$1 = |\det M(\alpha, \beta)| = |n_1 n_2 + n_1 n_3 + n_2 n_3|.$$

Since both n_1 and n_3 are positive, it is evident that the right-hand side of this equation is greater than 1 if n_2 is also positive, so n_2 must be negative, as claimed. When $n_2 = -1$, this equation can be written as $1 = |(n_1 - 1)(n_3 - 1) - 1|$, which means that $(n_1 - 1)(n_3 - 1)$ is equal to either 0 or 2. If both n_1 and n_3 are greater than 1, in which case this expression is non-zero, it follows immediately that $n_1 = 2$ and $n_3 = 3$, since we have assumed $n_1 \leq n_3$. \square

Proof of (a) of Proposition 3.1. Suppose that $M[n_1, n_2, n_3] \cong S^3$, n_1 and n_3 are strictly positive, and $n_2 \neq 0$. By Lemma 3.1, we know that $n_2 < 0$. We wish to prove that $n_2 = -1$. To do this, we consider the Whitehead graph for the Heegaard diagram of $M[n_1, n_2, n_3]$ discussed above. Our method of drawing $\Sigma_\alpha(\beta)$ is illustrated in Figure 10 for the simple case $n_1 = 1, n_2 = -1, n_3 = 1$. As in Section 2.2, we view the Heegaard surface Σ as the boundary of $F \times [-1, 1]$, where F is a surface of type $(0, 3)$ identified with the fiber surface for $L[n_1, n_2, n_3]$. Letting ϕ denote the corresponding monodromy, we compute $\phi(\gamma_1)$ and $\phi(\gamma_2)$ as before, where all arcs are thought of as lying in the

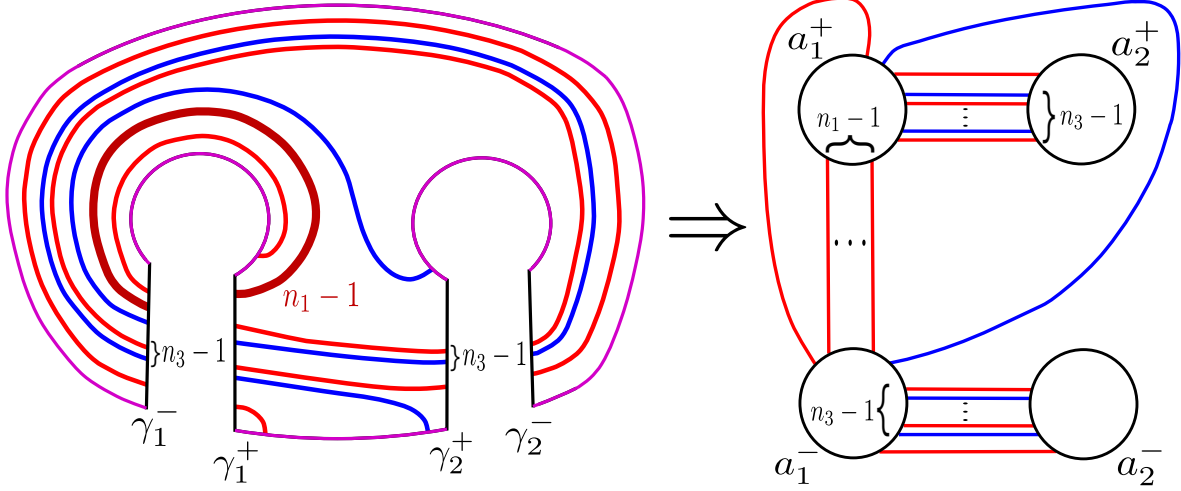


Figure 11: Constructing the Whitehead graph $\Sigma_\alpha(\beta)$ in the case $n_1, n_3 > 0, n_2 = -1$. On the right, the weights given to the bold arc and two pairs of parallel arcs indicate the number of times that they appear.

‘bottom’ $F \times \{-1\}$ of Σ . We then construct β_i and α_i from $\phi(\gamma_i)$ and a push-off of γ_i (respectively) as described in Section 2.2, and cut Σ along α_1 and α_2 to obtain Σ_α . In the figure, the boundary components of Σ_α arising from the cut along α_i are denoted by a_i^- and a_i^+ , labeled so that the arc in β_i which lies outside of $F \times \{-1\}$ runs parallel to an arc in a_i^+ .

This method of constructing the Whitehead graph $\Sigma_\alpha(\beta)$ is illustrated in Figures 11 and 12 for the pertinent values of n_1, n_2 , and n_3 . In each figure, the diagram on the left corresponds to the portion of the left side of Figure 10 which lies in the lower copy $F \times \{-1\} \subset \Sigma$ of F . While one can construct a picture of the other Whitehead graph $\Sigma_\beta(\alpha)$ directly, there is a way of viewing this process which

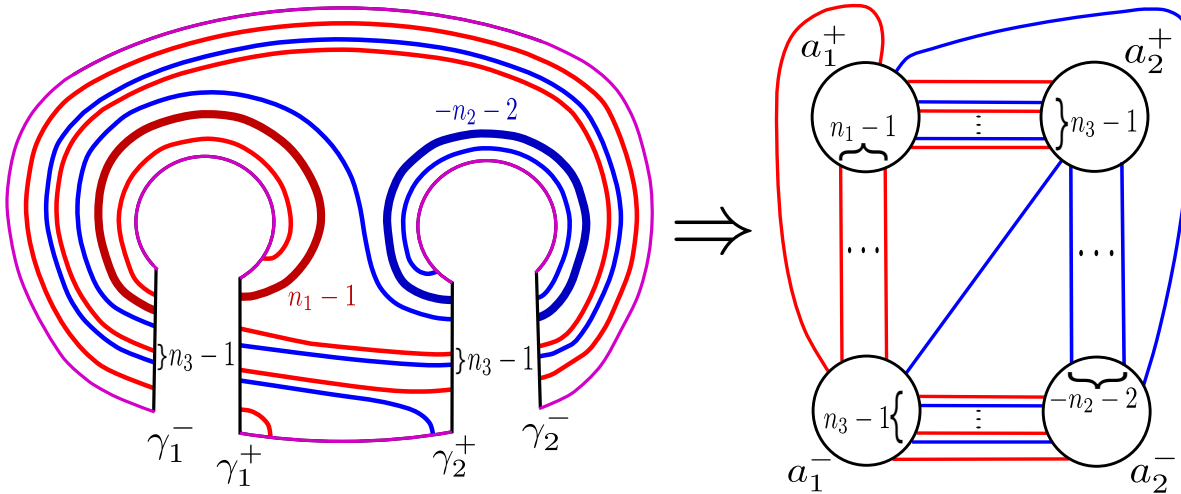


Figure 12: Constructing the Whitehead graph $\Sigma_\alpha(\beta)$ in the case $n_1, n_3 > 0, n_2 < -1$, where it does not contain a wave. On the right, the weights given to the two bold arcs and pairs of parallel arcs indicate the number of times that they appear.

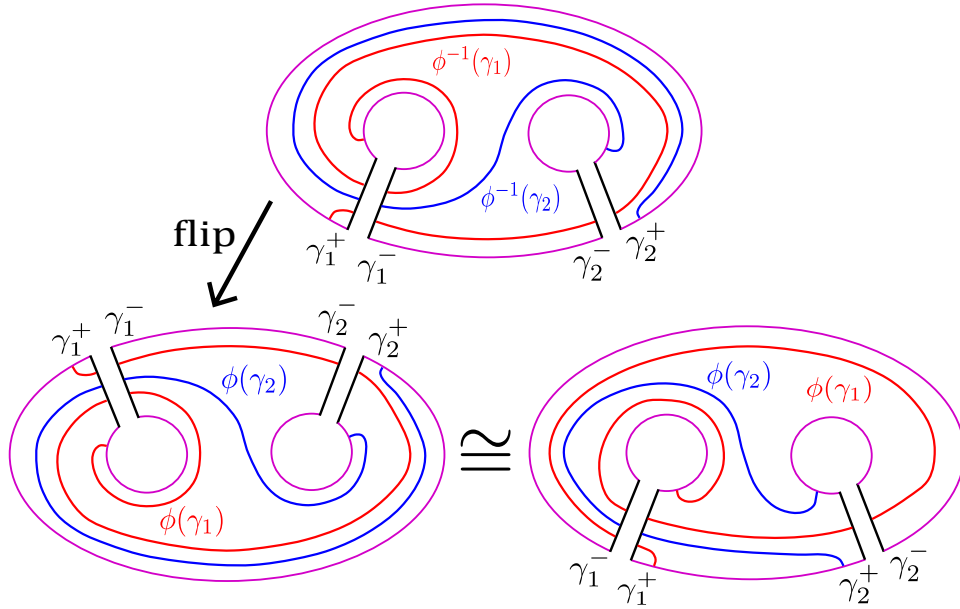


Figure 13: Going from the diagram in F used to construct $\Sigma_\beta(\alpha)$ (top) and that used to construct $\Sigma_\alpha(\beta)$ (bottom) in the case $n_1 = 1 = n_3$, $n_2 = -1$, the same one treated in Figure 10.

reveals a direct relationship between $\Sigma_\beta(\alpha)$ and $\Sigma_\alpha(\beta)$. Begin by applying $\phi^{-1} = T_1^{-n_1}T_2^{-n_2}T_3^{-n_3}$ simultaneously to all four arcs involved in the construction of $\Sigma_\alpha(\beta)$. We can reconstruct α_i and β_i from this new picture as before, as illustrated in Figure 5 of Section 2.2, but with $\phi^{-1}(\gamma_i)$ playing the role of $\phi(\gamma_i)$ and the roles of α_i and β_i interchanged. We then cut along β_1 and β_2 to obtain $\Sigma_\beta(\alpha)$.

Under appropriate labellings of the copies of β_i in Σ_β as b_i^+ and b_i^- for $i = 1, 2$, this construction reveals $\Sigma_\beta(\alpha)$ to be exactly the same as $\Sigma_\alpha(\beta)$ upon replacing b 's with a 's. To see this, note that the above procedure is tantamount to taking our original picture of F , with the arcs γ_i and $\phi(\gamma_i)$, flipping it over vertically, and then proceeding just as in the construction of $\Sigma_\alpha(\beta)$. The correspondence between the pictures in $F - (N(\gamma_1) \cup N(\gamma_2))$ leading to the Whitehead graphs is depicted in Figure 13 for the case $n_1 = 1 = n_3$, $n_2 = -1$. The upper diagram is that used to construct $\Sigma_\beta(\alpha)$, while the lower two diagrams are used to construct $\Sigma_\alpha(\beta)$.

In particular, we see that $\Sigma_\alpha(\beta)$ contains a wave if and only if $\Sigma_\beta(\alpha)$ does. By Theorem 2.1, $\Sigma_\alpha(\beta)$ must contain a wave if $M[n_1, n_2, n_3] \cong S^3$. However, as visible in Figure 12, $\Sigma_\alpha(\beta)$ does not contain a wave when $n_1 > 0$, $n_3 > 0$, and $n_2 < -1$, so it follows that $\Sigma_\beta(\alpha)$ also does not contain a wave. Combined with Lemma 3.1, this shows that if $n_1 > 1$, $n_3 > 1$, and $n_1 \leq n_3$, then $M[n_1, n_2, n_3] \cong S^3$ only if $n_2 = -1$. This proves Proposition 3.1 (a), and thereby proves the main theorem. \square

References

- [1] S. BAADER AND C. GRAF, *Fibred links in S^3* , *Expositiones Mathematicae*, 34 (2016), pp. 423–435.
- [2] D. BUCK, K. ISHIHARA, M. RATHBUN, AND K. SHIMOKAWA, *Band surgeries and crossing changes between fibered links*, *J. Lond. Math. Soc.*, 94 (2016), pp. 557–582.

- [3] J. ETNYRE, *Lectures on open book decompositions and contact structures*, in Floer homology, gauge theory, and low-dimensional topology, vol. 5 of Clay Math. Proc., Amer. Math. Soc., Providence, RI, 2006, pp. 103–141.
- [4] J. ETNYRE AND B. OZBAGCI, *Invariants of contact structures from open books*, Transactions of the American Mathematical Society, 360 (2008), pp. 3133–3151.
- [5] B. FARB AND D. MARGALIT, *A Primer on Mapping Class Groups*, Princeton University Press, Princeton, NJ, 2012.
- [6] D. GABAI, *Detecting fibered links in S^3* , Comm. Math. Helv., 61 (1986), pp. 519–555.
- [7] R. E. GOMPF AND A. I. STIPSICZ, *4-Manifolds and Kirby calculus*, vol. 20 of Graduate Studies in Mathematics, Amer. Math. Soc., Providence, RI, 1999.
- [8] F. GONZÁLEZ-ACUNA, *Dehn’s construction on knots*, Bol. Soc. Mat. Mexicana, 15 (1970), pp. 58–79.
- [9] J. HARER, *How to construct all fibered knots and links*, Topology, 21 (1982), pp. 263–280.
- [10] T. HOMMA, M. OCHIAI, AND M.-O. TAKAHISHI, *An algorithm for recognizing S^3 in 3-manifolds with Heegaard splittings of genus two*, Osaka J. Math, 17 (1980), pp. 625–648.
- [11] J. MEIER AND A. ZUPAN, *Genus two trisections are standard*, arXiv:1410.8133, (2014).
- [12] M. OCHIAI, *Heegaard-diagrams and Whitehead-graphs*, Math. Sem. Notes of Kobe Univ., 7 (1979), pp. 573–590.
- [13] J. SCHULTENS, *Introduction to 3-manifolds*, vol. 151 of Graduate Studies in Mathematics, Amer. Math. Soc., 2014.
- [14] J. STALLINGS, *Constructions of fibred knots and links*, in Algebraic and Geometric Topology, vol. 32 of Proc. Sympos. Pure Math, Amer. Math. Soc., 1978, pp. 55–59.